RAA 2018 Vol. **18** No. **9**, 112(10pp) doi: 10.1088/1674–4527/18/9/112

http://www.raa-journal.org *http://iopscience.iop.org/raa*

***R**esearch in*
***A**stronomy and*
***A**strophysics*

Photometry and spectroscopy of II Peg, IM Peg and UX Ari

Ajaz Ahmad Dar[1,2,3], Padmakar Singh Parihar[3] and Manzoor Ahmad Malik[1]

[1] Department of Physics, University of Kashmir, Hazratbal 190006 Srinagar-J&K, India; *mmalik@kashmiruniversity.ac.in*

[2] Department of Physics, Islamia College of Science and Commerce, Hawal, Srinagar-19002, J&K, India

[3] Indian Institute of Astrophysics, Koramagala-560034, Bangalore, India

Received 2018 March 22; accepted 2018 May 1

Abstract V band photometry of three RS CVn stars, II Peg, IM Peg and UX Ari, is carried out to study the physical properties of these variables. We verified the significant and regular optical photometric variability to be present in all three stars. The strong photometric variability and emission of Hα and Ca II H & K using high resolution optical spectroscopy with the Hanle Echelle Spectrograph (HESP), which operates in conjunction with the Himalayan Chandra Telescope, verify the strong chromospheric activity which is present in RS CVn stars. The photometric studies of II Peg, UX Ari and IM Peg were subjected to light curve analysis for spot parameters using a two-starspot model.

Key words: RS CVn: star spots: chromospherically active

1 INTRODUCTION

RS Canum Venaticorm (RS CVn) type stars are chromospherically active binary systems with large starspots, strong chromospheric plages, coronal X-ray and microwave emissions, as well as strong flares in the optical, radio and other spectral regions (Tautvaišienė et al. 2012; Hall 1976). The term RS CVn binary is used for a system which shows the presence of strong Ca II H & K and H emission in the spectrum. Variable light curves arise primarily due to rotational modulation of the stellar light by large starspots on the surface of the cooler component. The rotation of the star, which is usually synchronous with the orbital revolution, produces a distortion wave as the darker regions are turned toward or away from the observer. The phase variability causes the distortion wave to migrate relative to the orbital period or (if the system eclipses) relative to the eclipse light curve. This distortion wave is believed to be due to starspot groups, which are darker regions near the equator of the star (Ayman 2013). The binary usually consists of one hotter component of the spectral type F or G and luminosity class V or IV. The secondary cooler companion is usually a subgiant or giant massive K-type star. Both stars typically lie well inside their Roche lobe. RS CVn stars show photometric variability other than that which may be due to eclipses. The variability in amplitude is attributed to the varying area of the spots, and variability in phase of the distortion wave is expected due to differential rotation of the star, which affects the position of the starspot region relative to the comparison star and orbital phase (Ulvås & Henry 2003). Discoveries of newly identified RS CVn binary systems are important for understanding the associated underlying physical parameters like rotation, age, metallicity, etc., which are involved in generating and sustaining their strong chromospheric and coronal activity (Padmakar & Pandey 1999).

1.1 II Peg

II Pegasi (II Peg, HD 224085), ranked among the most active RS CVn stars, is an ideal target to study stellar activities and flares, since intense and long lasting flares have been frequently detected from this system at all wavelengths (Byrne et al. 1995). II Peg is a single lined spectroscopic binary with a period of 6.72 days composed of a primary spectral type K2 IV-V and an unobserved companion (Covino et al. 2000). Its photometric variability was first discussed by Chugainov (1976) and its orbit was first determined by Sanford (1921) and Vogt

(1981). Byrne et al. (1995) found no trace of a companion in either the photospheric or chromospheric spectrum, leading to their conclusion that it is a low luminosity object, possibly a very late-type M dwarf. II Peg has been widely studied in a wide range of wave bands apart from the optical, and it was reported that II Peg undergoes frequent flaring in all these wave bands.

1.2 IM Peg

IM Pegasi (IM Peg), a chromospherically active and spotted binary system – the guide star of the Gravity Probe B mission to study the consequences of General Relativity, is classified as a spectroscopic binary RS CVn star with a period of about 24.69 days (Zellem et al. 2010). Herbst (1973) classified it as a spectral type of KI IV-III with strong CaII H and K emission. Also, the primary shows signs of both photospheric and chromospheric activity and has rotational velocity of $v \sin i = 28\,\mathrm{km\,s^{-1}}$ (Korhonen et al. 2010). IM Peg undergoes light variations up to 0.3 mag in the V band and these variations arise from the rotation modulation associated with inhomogeneous areal surface coverage of starspots (Strassmeier 1997; Padmakar & Pandey 1999). The photometric variations were attributed to starspot activity. Titanium oxide (TiO) photometry reported by Zellem et al. (2010) allows us to estimate the absolute spot coverage as well as the magnitude of IM Pegs. Marsden et al. (2007), using a Doppler imaging (DI) technique, found a polar spot which can considerably reduce IM Pegs' light without producing phased light variations.

1.3 UX Ari

UX Arietis (UX Ari) is a non-eclipsing type triple-lined system, where the two main components constitute a double lined spectroscopic RS CVn binary system with hot G5V primary and active cool K0 IV secondary star (Padmakar & Pandey 1996, 1999). The oldest photometric observations of UX Ari to be found in the literature are those presented by Hall et al. (1975). Their light curve had an amplitude of $\Delta_V = 0.1$ magnitude and a period of 6.43791 days as determined spectroscopically by Carlos & Popper (1971). The wave amplitude of this star is found to vary within the range $\sim 0.02 - 0.3$ magnitude over the last three decades. The last observations of UX Ari were done by Ulvås & Henry (2003). We monitor this object to compare the results with previously reported data spanning 30 years and see the variations in period, amplitude and other stellar properties like starspot activities. The spot distribution of UX Ari has been investigated using the starspot model.

In this paper, we discuss the V-band optical photometry of RS CVn stars II Peg, IM Peg and Ux Ari that was acquired with an Automated Extinction Monitor (AEM), which is part of a small telescope setup located near the village of Hanle in northern India. Such data are used to deduce the distribution of starspots on these stars. In addition, we present high resolution spectroscopy, acquired with the Hanle Echelle Spectrograph (HESP) which operates in conjunction with the 2-m Himalayan Chandra Telescope (HCT). These spectroscope data contain a number of chromospheric diagnostics lines, including Hα. We will use the data to describe and discuss evidence for localised features in their chromospheres.

2 OBSERVATIONS AND DATA REDUCTION TECHNIQUES

Small optical ground based telescopes can provide valuable information regarding the photometric variability, brightness, structure and character of celestial objects. These can also provide an effective means of tracing the evolution of starspots on chromospherically active stars (Padmakar & Pandey 1999). These smaller telescopes equipped with modern detectors, if housed at high altitude observing sites, can remarkably improve night sky observations (Pandey 2006). The RS CVn monitoring of II Peg, IM Peg and UX Ari was done by using the AEM at the high altitude observatory near Hanle. The AEM, operational since 2012, is comprised of a wide field Nikon 300 mm f/4 telephoto lens, a yoke mount equatorial tracking system and a thermoelectrically cooled large format U32 Apogee CCD Camera having a field of view of about $2.8^\circ \times 1.9^\circ$, pixel area of 2184×1472 and full well capacity of about $55\,000\,\mathrm{e^-}$. A broadband (Johnson V) bandpass filter is placed between the CCD and the telephoto lens. The device is working under a tilted sliding roof enclosure which is controlled by computers (Padmakar et al. 2015). The photometric observations of IM Peg were carried out from 2016 November 1 to 2016 December 31. Observations of UX Ari were acquired from 2016 November 1 to 2016 November 30 and II Peg was observed from 2016 November 1 to 2016 December 31, in V-filter only. The exposure times given for II Peg, IM Peg and UX Ari are 4 s, 2 s and 3 s respectively. The data reduction process was started by combining individual bias frames into an average image (master bias). Then average bias was subtracted from science images and flat fields, and combined with individual flat fields into an average image. The average flat field was normalised using imstat and imarith tasks. Finally, we divided the science images by the normalised flat field. The IRAF tasks used for cleaning of images were zerocombine, ccdproc, flatcombine, imstat and imarith, and cosmic ray removal was performed with the crutil package. Alignment of images was done by using the geomap and geotran tasks. The beauty of these tasks lies in the fact that they also take care of rotation in the image and ensure alignment within a 0.3 pixel range. Instrumental magnitudes were obtained by using the apphot task in IRAF.

3 OPTICAL PHOTOMETRY OF II PEG, IM PEG AND UX ARI

We employed the ensemble photometry technique for finding the variables and non-variables in terms of their standard deviations. The CCD ensemble photometry technique is used to calculate the difference between the instrumental magnitude of a program star and a comparison magnitude obtained from the sum of intensities of about a dozen brighter stars which appear in each exposure in the series. A variation of CCD ensemble photometry arises when the number and identity of the comparison stars vary significantly from exposure to exposure (Honeycutt 1992). After running python codes, we had little indication as to whether a variable star has been included in the ensemble stars until we completed many iterations of the code. To identify and remove the variables from the ensemble, we examined a few basic statistics calculated for each light curve. Those stars in the ensemble whose light curves exhibit large standard deviations were removed from the ensemble. Among the rejected stars are the variables, crowded stars and stars with cosmic rays in their aperture. The ensemble stars found to be variable or having cosmic ray contamination as mentioned above are removed from the ensemble and the process is repeated until all the ensemble stars are found to be non-variable. Photometric variability in light curves of three RS CVn stars, II Peg, IM Peg and UX Ari, is shown in Figure 1, Figure 2 and Figure 3 respectively. The phases are computed with the ephemeris shown in Table 1. From the phase diagrams it is evident that observations cover the entire phase.

4 SPOT MODELS

Photometric variations provide valuable information regarding the physical characteristics such as size, location and effective temperature of the starspots. To evaluate the geometric parameters of starspots from the observed light curves, we used the computer program of Padmakar & Pandey (1999) based on the Dorren (1987) algorithm with some modifications for analytical formulation of circular spots. The computer program has a graphical interface using PGPLOT5 plotting subroutines, which allows the user to judge the quality of a fitting and improve upon it. The important purpose of the program is to (i) determine the geometry of the spot parameters, (ii) perform long term analysis of several years of photometric data and (iii) generate synthetic light curves for any number of discrete spots either keeping the temperature and limb darkening coefficients constant or varying them. The program uses a least squares curve fitting technique based on minimisation of χ^2 (Barway 2005). Earlier starspot models used were those of Bopp & Evans (1973), Budding (1977), Dorren (1987) and Strassmeier et al. (1988). Our aim is to look for the change in shape and amplitude of light curves for these binaries. The traditional two starspot model has been used to obtain the spot parameters from the observed light curves of the stars. For spot modeling, we have kept ΔT constant to evaluate the flux ratio between the spot and photosphere using a blackbody approximation with $\Delta T = 1000\,\mathrm{K}$. Also, the limb darkening coefficient and inclination were kept constant.

Table 1 Basic Parameters of These RS CVn Stars (Padmakar & Pandey 1999)

Star	Spectral type	$V_{\max}$	Ephemeris
II Peg	K2 IV	7.306	2443030.239+06.724183 E^1
IM Peg	K1 V	5.630	2422230.992+24.64900 E^3
UX Ari	K0 IV	6.500	2440133.766+06.43791 E^2

The best fit spot parameters with their uncertainties are shown in Table 2, where i = orbital inclination, λ = longitude, β = latitude, γ = radius and γ_p = radius of polar spot. Units of all these parameters are in degrees and ΔT = temperature difference between stellar photosphere and starspots. Using our data (2016) along with photometric data from the literature, including Strassmeier et al. (1989), Catania APT Archive[1], Eaton et al. (1983), Sarma & Prakasa Rao (1984), Mohin & Raveendran (1993), etc., we have analyzed light variations of three RS CVn stars, namely II Peg, UX Ari and IM Peg, to investigate the characteristics and evolution of regions considered as spotted.

[1] *http://webusers.ct.astro.it/sme/web/apt/target-list.html*

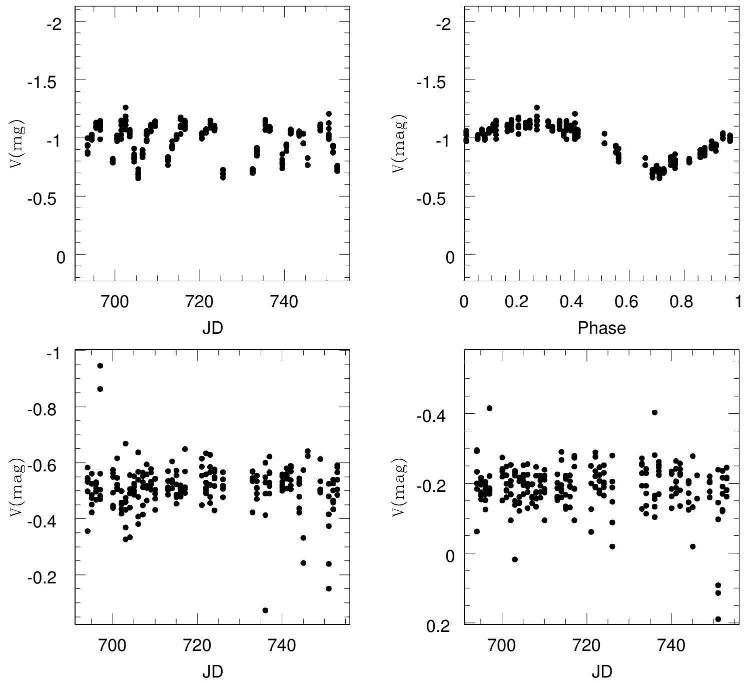

Fig. 1 Light curve of II Peg: Upper two plots show differential magnitude vs. Julian date (JD), and differential magnitude vs. phase. Lower two plots display differential magnitude of comparison stars vs. JD.

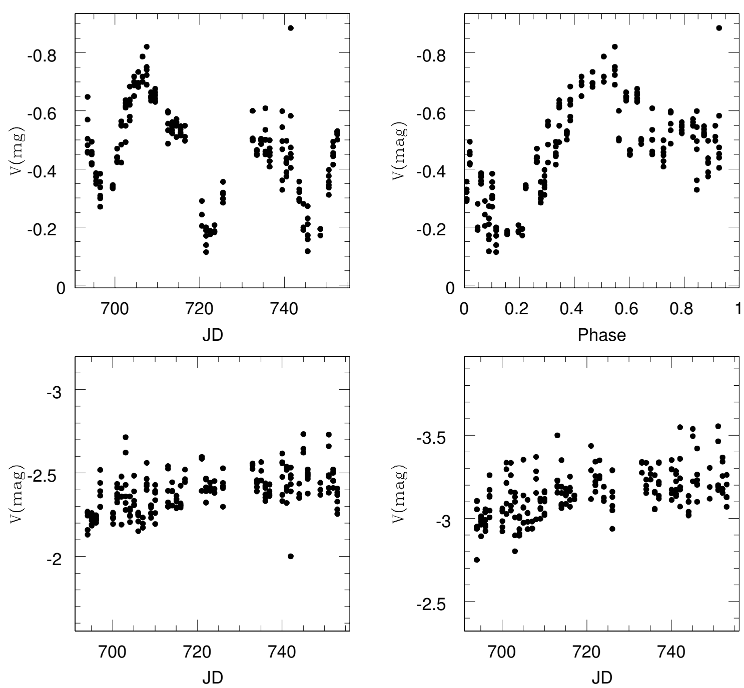

Fig. 2 Light curve of IM Peg: Upper two plots show differential magnitude vs. JD, and differential magnitude vs. phase. Lower two plots display differential magnitude of comparison stars vs. JD.

Figures 4 to 6 show synthetic light curves represented by solid lines. The observational data are represented by dots. It is obvious that the agreement between synthetic light curves and observational data is very good.

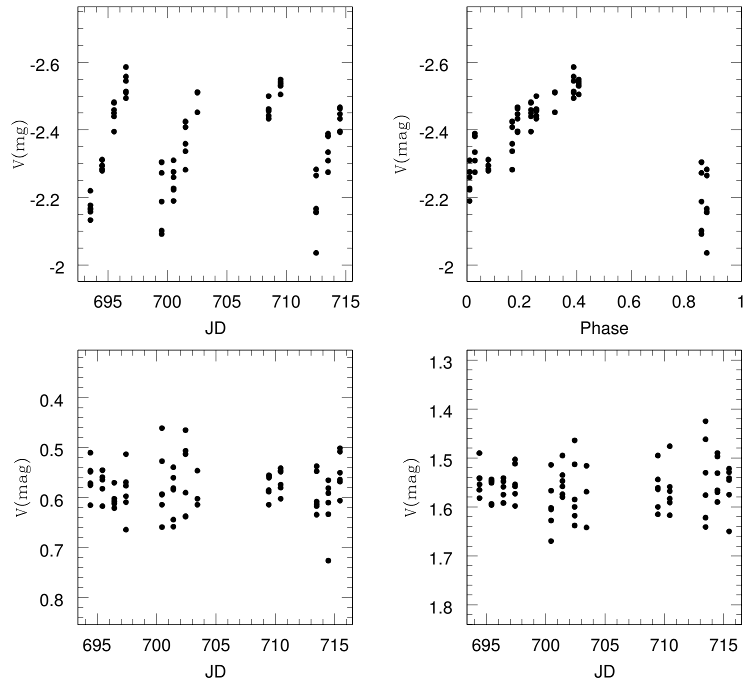

Fig. 3 Light curve of UX Ari: Upper two plots show differential magnitude vs. JD, and differential magnitude vs. phase. Lower two plots display differential magnitude of comparison stars vs. JD.

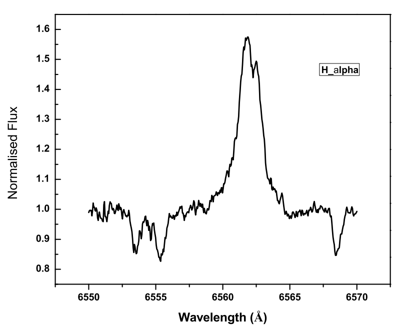

(a) Observed H_α in II Peg

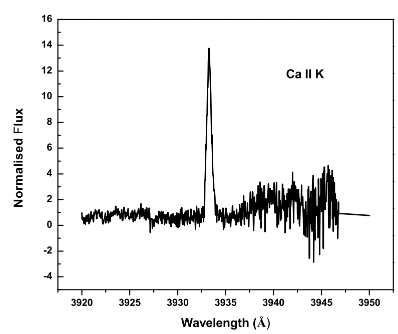

(b) Observed CaII K in II Peg

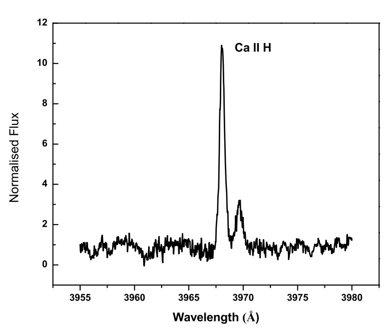

(c) CaII H in II Peg

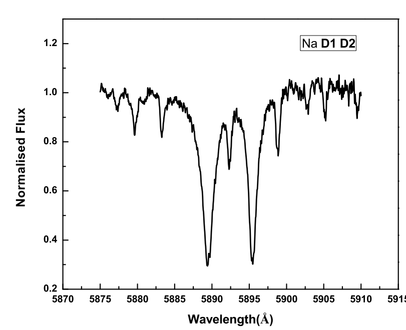

(d) Na D1 D2 lines in II Peg

Fig. 4 Chromospheric emission lines of II Peg.

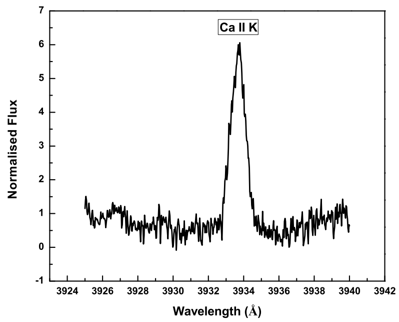

(a) Observed CaII K in IM Peg

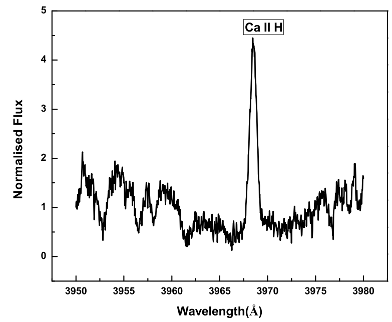

(b) Observed CaII H in IM Peg

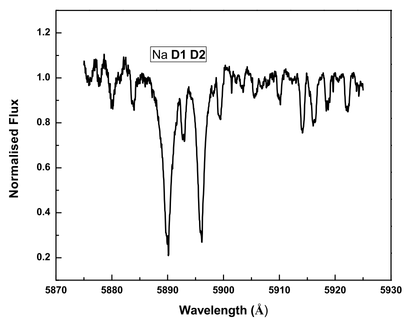

(c) Na D1 D2 lines in IM Peg

Fig. 5 Chromospheric emission lines of IM Peg.

5 HIGH RESOLUTION OPTICAL SPECTROSCOPY

Optical spectroscopy of IM Peg, II Peg and UX Ari was carried out on 2017–01–19 with HESP that operates with the 2m HCT. The integration times ranged from 200 s to 600 s. The spectrograph has wavelength coverage from 350 nm to 1000 nm on a single detector over 64 orders, resolution ranging from 30 000 to 60 000, two fibres: star-sky observations and provision for simultaneous reference observations using a ThAr lamp, and non-referenced mechanical stability: 20 m s^{-1} and reference velocity precision of 20 m s^{-1} (Chanumolu et al. 2015). The detector used is a 4k×4k E2V CCD231-84, with 15 micron pixel size, read noise 3.66 and gain 2.8 photons per data-number. Byrne et al. (1998) suggested that the non-uniform distribution of magnetic heating on RS CVn stars leads to variability in these stars. They also detected flux in suitable chromospheric and coronal radiations as the star rotates, i.e. rotational modulation. The spectroscopic observations were reduced and analysed using the spectroscopic reduction package Echelle in IRAF. After correction for bias, flat, background and dispersion, all spectra were normalised by fitting a spline function to the continuum, and equivalent widths (EWs) for emission lines were extracted. High resolution echelle optical spectroscopy of all three RS CVn stars shows strong emission of Ca II H & K and absorption of Na D1 and D2 lines as displayed in Figure 7 to 9. In the case of II Peg, strong emission of Hα, which is a good indicator of chromospheric activity, can be seen in Figure (4c). The Hα emission in case of II Peg is assumed to be stronger than the local continuum. The EWs of Ca II K and Ca II H suggest strong emission for all the three RS CVn stars except for Hα, which was not seen in IM Peg and UX Ari for this observing run. Hα emission of II Peg by comparison with Byrne et al. (1998) indicates its variations over a slightly larger range, i.e. –1.3 Å. It is assumed that the larger value of EW (Hα) may be likely due to flare. Measurement of the EW of a given line needs the determination of area bordered by the line profile and the continuum. This area is transformed to a rectangular line with depth of 1.0. The width of this rectangle is called the EW. Emission lines by definition have a negative

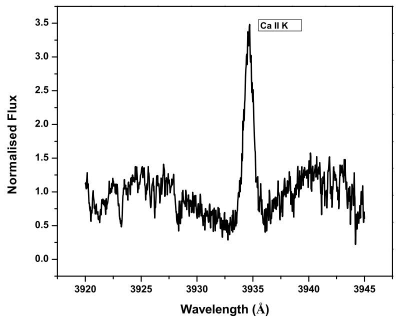

(a) Observed CaII K in UX Ari

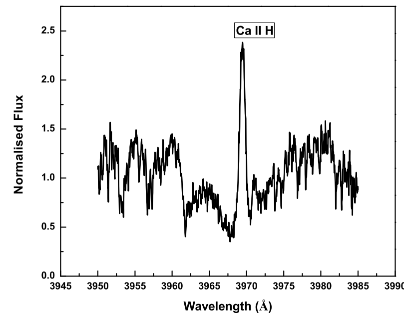

(b) Observed CaII H in UX Ari

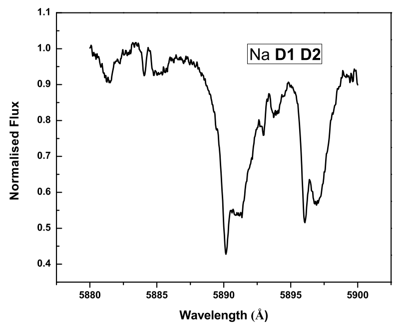

(c) Na D1 D2 lines in UX Ari

Fig. 6 Chromospheric emission lines of UX Ari.

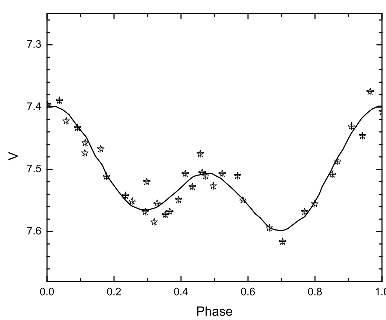

(a) year 1985.67

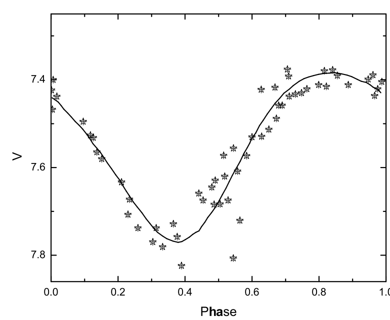

(b) year 1989.83

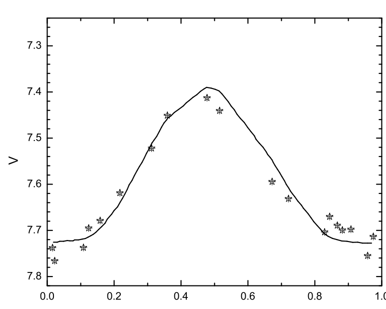

(c) year 1998.98

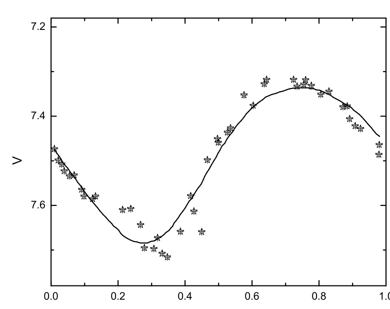

(d) year 2016.99

Fig. 7 V light curve of II Peg using spot model.

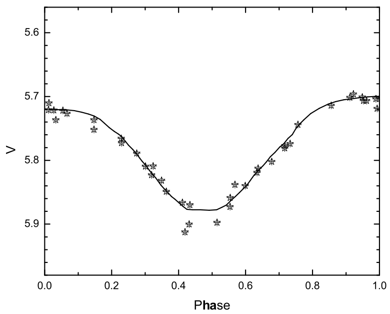

(a) year 1984.98

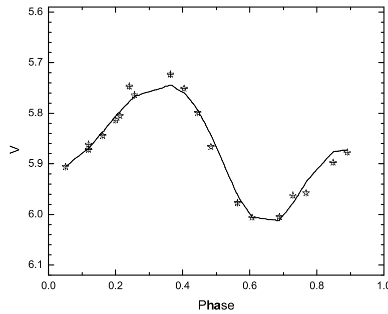

(b) year 1988.51

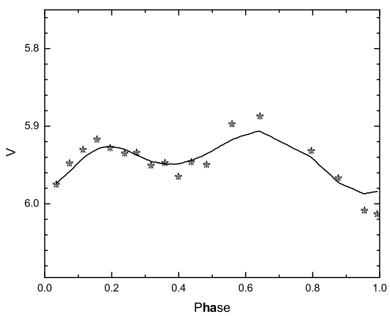

(c) year 1998.94

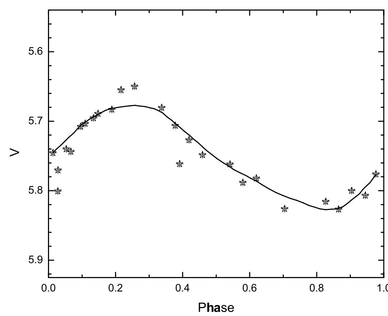

(d) year 2016.99

Fig. 8 V light curve of IM Peg using spot model.

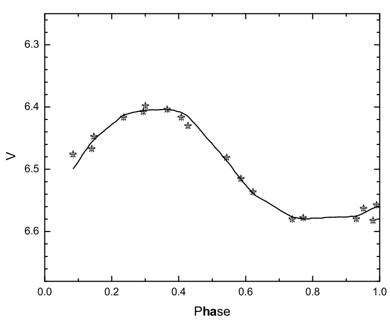

(a) year 1988.16

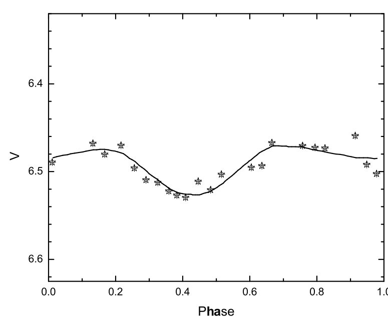

(b) year 1991.17

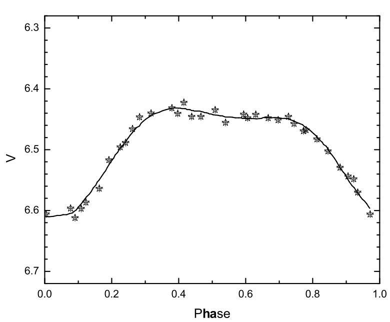

(c) year 1996.17

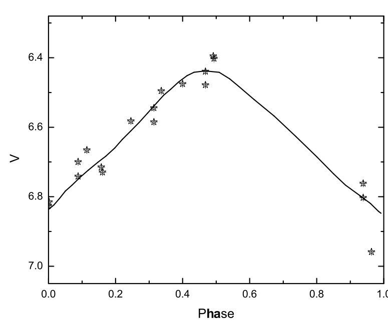

(d) year 2016.92

Fig. 9 V light curve of UX Ari using spot model.

Table 2 Spot Parameters of RS CVn Stars

Star	Avg. JD	Year	λ_1	β_1	γ_1	λ_2	β_2	γ_2	γ_p	Total Area (%)
II Peg	2446229.00	1985.67	253.86±3.38	27.35±2.18	32.84±0.29	99.46±4.20	8.62±2.67	37.38±0.32	14.49±0.12	19.85±0.22
	2447102.50	1987.92	26.49±1.92	30.42±0.65	21.05±0.34	190.33±5.3	21.14±1.56	29.30±0.93	18.5±0.12	12.32±0.41
	2447430.00	1988.75	69.28±0.69	37.64±0.39	29.48±0.14	141.47±3.90	8.57±2.43	28.02±0.46	15.94±0.13	14.26±0.20
	2447808.50	1989.83	70.22±0.48	24.14±0.20	22.57±0.15	153.81±0.66	14.61±0.37	38.73±0.13	21.81±0.09	18.40±0.09
	2448415.50	1991.50	9±3.81	30.21±1.21	17.39±0.44	186.67±8.55	7.32±6.51	25.57±0.62	28±0.13	13.04±0.27
	2448883.50	1992.75	278.78±2.18	30.88±0.66	11.99±0.42	183.08±2.77	10.63±3.6	26.94±0.97	31.04±0.17	13.67±0.20
	2450075.00	1995.99	13.90±1.31	29.16±0.51	19.68±0.41	168.88±2.11	12.66±1.29	33.30±0.31	27.63±0.14	16.83±0.20
	2451168.00	1998.98	296.38±5.45	29.45±1.54	35.16±0.32	56.12±1.02	6.57±0.36	43.06±0.25	16.44±0.14	24.63±0.22
	2457723.50	2016.99	273.87±0.25	33.93±0.73	36.67±0.27	221.70±3.70	9.66±1.45	5.82±0.15	5.11±0.07	10.35±0.14
IM Peg	2443848.50	1978.99	237.05±28.76	25.79±6.63	10.36±0.38	161.03±1.09	43.15±1.26	21.01±0.19	25.03±0.23	9.06±0.12
	2446045.00	1984.98	353.19±0.67	36.78±2.49	20.85±0.11	260.05±3.80	−2.30±14.14	15.21±0.47	18.70±0.12	7.67±0.12
	2446590.00	1986.50	182.65±12.46	9.85±10.47	20.30±0.20	251.99±7.10	−8.09±4.95	20.53±0.16	21.95±0.48	9.91±0.18
	2447315.00	1988.51	7.62±1.06	34.22±1.97	20.46±0.2	232.71±0.65	10.97±1.04	28.39±0.29	29.60±0.30	15.69±0.19
	2450435.00	1996.99	198.59±0.02	5.98±0.39	28.17±0.06	279.69±0.08	10.95±1.20	29.57±0.10	39.72±0.11	23.98±0.08
	2451149.00	1998.99	342.94±10.98	5.52±7.75	13.16±0.35	140.69±0.47	6.64±0.84	10.80±0.34	47.5±0.21	18.42±0.16
	2457723.50	2016.99	356.30±0.04	22.96±2.14	33.27±2.48	254.10±0.13	–1.54±0.09	22.16±0.04	6.81±0.22	12.24±0.19
Ux Ari	2443080.00	1976.83	136.06±2.91	38.12±12.62	11.49±0.39	264.83±1.15	−14.56±10.94	21.52±0.75	40.22±0.33	16.31±0.32
	2447205.00	1988.16	337.3±0.84	33.3±2.96	23.08±0.12	237.8±1.85	1.42±2.23	23.53±0.48	20.59±0.54	11.35±0.24
	2448310.00	1991.17	17.48±34.02	30.72±48.02	6.55±1.04	155.52±5.01	11.50±8.33	14.59±0.52	32.41±0.31	9.72±0.21
	2449037.50	1993.16	5.84±2.5	29.61±38.16	26.43±0.09	134.82±9.64	6.38±7.66	22.39±0.38	14.36±0.38	10.56±0.15
	2450046.00	1995.92	8.34±1.76	34.09±1.73	21.97±0.08	230.14±8.12	8.36±0.93	11.72±0.31	26.02±0.26	9.74±0.12
	2450123.50	1996.17	12.56±1.70	38.20±1.75	24.25±0.09	212.76±25.8	−1.84±10.69	10.06±1.09	25.48±0.24	10.05±0.19
	2457704.50	2016.92	54.22±2.65	45.54±2.12	31.62±0.27	300.38±0.60	29.95±0.15	40.47±0.08	10.74±0.31	20.26±0.14

EW. The measurement is sensitive to continuum placement. Extremely shallow lines give a large error in EW (Vrancken et al. 1997). EWs are often used in abundance analysis. A good check of correct normalisation is the comparison of EWs for spectral lines of the same element in different spectral regions (Hensberge et al. 2000). The EWs are listed in Table 3.

Table 3 Basic Parameters of These RS CVn Stars

EWs in Å					
Object	CaII K	CaII H	Na D1	Na D2	Hα
II Peg	−14.51	−5.79	1.257	1.001	−1.317
IM Peg	−15.11	−4.971	1.259	1.042	–
Ux Ari	−4.938	−2.693	1.331	0.8754	–

6 CONCLUSIONS

In this paper, we have presented comprehensive ensemble photometric results of three important RS CVn stars: II Peg, IM Peg and Ux Ari with spot distribution covering over thirty years of data including our recent observations in the year 2016. Variation in light curves using a starspot model is evident from year to year. In the case of II Peg, the total spot area shows significant variation except for the years 1991 and 1992. From Table 2, for the year 2016, the radius of the polar spot of II Peg is very small in comparison to other years. The latitude distribution of starspots is found to be wide and some spots are located at intermediate latitude. Although II Peg is the most active among these RS CVn stars, its companion is of such low luminosity that it has neither been found in the photospheric nor the chromospheric spectrum. However, long term high resolution spectroscopic observation of II Peg in the future may provide some clue about its companion and hence one may be able to better understand the dynamical properties like mass and inclination (Byrne et al. 1995).

IM Peg shows significant evolution of the spot pattern from epoch to epoch. The distribution of spot longitudes and latitudes is presented in Table 2. For UX Ari, large variation in total spot area is observed in 1976 and 2016, whereas data show little variation in total spot area from 1988 to 1996. It is assumed that the differential rotation, which is due to internal magnetic field, causes little variation in latitude spots. It appears that polar spots are more or less uniformly distributed in longitudinal belts. Thirty years of data in the framework of the starspot model for Ux Ari reveal that the spot activity shows periodicity. It would be interesting to make a comparison between the two spot model and the surface maps obtained from DI for a more accurate estimation of errors. Chromospheric activity was verified using high resolution spectroscopy with strong emission of Ca II K and Ca II H lines.

In the case of II Peg, a prominent Hα emission line is clearly visible and may be an important tracer of magnetic heating because of its abundance. The II Peg Hα line EW is -1.317, which is slightly over the range of Byrne et al. (1998) and Liu & Tan (1987). For IM Peg and UX Ari, the Hα emission remains within or well below the continuum. The reason may be that absorption in the photosphere is so deep that the Hα line is not able to come out above the continuum. The EW of Ca II K and Ca II H indicates strong emission for all the three objects. Also, our spectroscopic observations show clear absorption lines of Na D1 and Na D2 with stronger fill in. High resolution spectroscopic observations reveal that II Peg, IM Peg and Ux Ari are indeed very interesting objects. In the future, continuous high resolution spectroscopic observations of II Peg, IM Peg and Ux Ari can provide better understanding of spectroscopic parameters like metallicity, excitation potential, temperature, abundances, etc.

Acknowledgements One of the authors, Ajaz Ahmad Dar, is thankful to the University Grants commission, New Delhi for awarding the Faculty Development Programme (teacher fellowship for pursuing Ph.D.) and Islamia College of Science and Commerce, Srinagar for deputation to the University of Kashmir for the said programme. Ajaz Ahmad Dar is thankful to the Director of the Indian Institute of Astrophysics (IIA), Bangalore for hosting him at IIA for extended periods.

References

Ayman, M. A. 2013, Thesis Photometric Analysis of RS CVn and Eclipsing Binary Stars, Ph. D. Thesis, Astronomy and Space Department, College of Science, University of Baghdad, Iraq

Barway, S. 2005, A Study of Stellar Activity in Chromospherically Active Stars, Ph. D Thesis, Pt. Ravishankar Shukla University, Raipur, India

Bopp, B. W., & Evans, D. S. 1973, MNRAS, 164, 343

Budding, E. 1977, Ap&SS, 48, 207

Byrne, P. B., Panagi, P. M., Lanzafame, A. C., et al. 1995, A&A, 299, 115

Byrne, P. B., Abdul Aziz, H., Amado, P. J., et al. 1998, A&AS, 127, 505

Carlos, R. C., & Popper, D. M. 1971, PASP, 83, 504

Chanumolu, A., Jones, D., & Thirupathi, S. 2015, Experimental Astronomy, 39, 423

Chugainov, P. F. 1976, Izvestiya Ordena Trudovogo Krasnogo Znameni Krymskoj Astrofizicheskoj Observatorii, 54, 89

Covino, S., Tagliaferri, G., Pallavicini, R., Mewe, R., & Poretti, E. 2000, A&A, 355, 681

Dorren, J. D. 1987, ApJ, 320, 756

Eaton, J. A., Hall, D. S., Henry, G. W., et al. 1983, Ap&SS, 89, 53

Hall, D. S. 1976, Multiple Periodic Variable Stars, 1AU Colloquium no. 29 (Budapest), part 1, 297

Hall, D. S., Montle, R. E., & Atkins, H. L. 1975, Acta Astronomica, 25, 125

Hensberge, H., Pavlovski, K., & Verschueren, W. 2000, A&A, 358, 553

Herbst, W. 1973, A&A, 26, 137

Honeycutt, R. K. 1992, PASP, 104, 435

Korhonen, H., Weber, M., Wittkowski, M., Granzer, T., & Strassmeier, K. G. 2010, in IAU Symposium, Vol. 264, Solar and Stellar Variability: Impact on Earth and Planets, ed. A. G. Kosovichev, A. H. Andrei, & J.-P. Rozelot, 267

Liu, X.-f., & Tan, H.-s. 1987, Chinese Astronomy and Astrophysics, 11, 64

Marsden, S. C., Berdyugina, S. V., Donati, J.-F., Eaton, J. A., & Williamson, M. H. 2007, Astronomische Nachrichten, 328, 1047

Mohin, S., & Raveendran, A. V. 1993, A&A, 277, 155

Padmakar, & Pandey, S. K. 1996, Ap&SS, 235, 337

Padmakar, & Pandey, S. K. 1999, A&AS, 138, 203

Padmakar, P., Sharma, T. K., Surendran, A., et al. 2015, Journal of Physics: Conference Series, 595, 012025

Pandey, S. K. 2006, IAU Special Session, 5, #36

Sanford, R. F. 1921, ApJ, 53, 201

Sarma, M. B. K., & Prakasa Rao, B. V. N. S. 1984, Journal of Astrophysics and Astronomy, 5, 159

Strassmeier, K. G., Hall, D. S., Eaton, J. A., et al. 1988, A&A, 192, 135

Strassmeier, K. G., Hall, D. S., Boyd, L. J., & Genet, R. M. 1989, ApJS, 69, 141

Strassmeier, K. G. 1997, A&A, 319, 535

Tautvaišienė, G., Barisevičius, G., Berdyugina, S., Ilyin, I., & Chorniy, Y. 2012, Proceedings of the International Astronomical Union, 8, 207

Ulvås, A. V., & Henry, G. W. 2003, A&A, 402, 1033

Vogt, S. S. 1981, ApJ, 247, 975

Vrancken, M., Hensberge, H., David, M., & Verschueren, W. 1997, A&A, 320, 878

Zellem, R., Guinan, E. F., Messina, S., et al. 2010, PASP, 122, 670